Validation of a simple model for the morphology of the T wave in unipolar electrograms

Mark Potse[1,2,3,4], Alain Vinet[1,4], Tobias Opthof[2,5], and Ruben Coronel[2]

[1] Institute of Biomedical Engineering, Université de Montréal, Montreal, Quebec, Canada
[2] Department of Experimental Cardiology, Center for Heart Failure Research, Academic Medical Center, Amsterdam, The Netherlands
[3] Interuniversity Cardiology Institute of the Netherlands, Utrecht, The Netherlands
[4] Research Center, Sacré-Coeur hospital, Montreal, Quebec, Canada
[5] Department of Medical Physiology, University Medical Center, Utrecht, The Netherlands.

This is a compact version of the manuscript for the following paper: Potse M, Vinet A, Opthof T, and Coronel R. Validation of a simple model for the morphology of the T wave in unipolar electrograms. Am. J. Physiol. Heart Circ. Physiol. (accepted for publication) 2009.

Abstract

Local unipolar electrograms (UEG) permit assessment of local activation and repolarization times at multiple sites simultaneously. However, UEG-based indices of local repolarization are still debated, in particular for positive T waves. Previous experimental and computer modeling studies have not been able to terminate the debate. In this study we validate a simple theoretical model of the UEG and use it to explain how repolarization statistics in the UEG relate to those in the action potential. The model reconstructs the UEG by taking the difference between an inverted local action potential and a position-independent "remote" signal. In normal tissue, this extremely simple model predicts T-wave morphology with surprising accuracy, while explaining in a readily understandable way why (1) the instant of repolarization is always related to the steepest upstroke of the UEG, both in positive and negative T waves, and (2) positive T waves are related to early-repolarizing sites whereas negative T waves are related to late-repolarizing sites.

Introduction

Measurement of repolarization time from the unipolar electrogram (UEG) is important for clinical studies of repolarization abnormalities, as well as for experimental studies. It is therefore important to understand how the T wave in the electrogram is generated, and how it relates to local repolarization time. The ongoing debate on repolarization measurement in positive T waves [8, 9, 23, 47, 48] demonstrates that this understanding is incomplete.

Wyatt et al. [45] proposed to use the instant of steepest upstroke (T_{up}) of the T wave in the UEG as an index of local repolarization. Several studies have confirmed the validity of this method theoretically [5, 6, 17, 34] and experimentally [3, 8, 17, 21]. Others have proposed that for positive T waves the instant of steepest downstroke (T_{down}) should be used [2, 13, 46]. The T-wave apex has also been used as an estimate for repolarization time [32].

The current mechanistic insight in the relation between T_{up} and repolarization is based on theoretical studies in a one-dimensional cable model [5, 6, 17, 34]. This explanation cannot be easily extended to arbitrary repolarization patterns in the 3-D heart. Numerical evaluations with realistic 3-D heart models have confirmed that theoretically T_{up} is the best index of repolarization even in the complex situation of a complete 3-D heart [5, 6, 28, 29], but the overwhelming complexity of the computational techniques does not allow for a clear explanation.

We propose a simple UEG model that is more suitable to give insight in repolarization phenomena. This model approximates the UEG by a linear combination of the local action potential (AP) and a position-independent signal which we name the "remote component." The purpose of this paper is to demonstrate that this model is accurate enough to predict the most important repolarization statistics, and that it can be used to understand how these statistics relate to the underlying AP. To show the validity and limitations of the simple model, simulated UEGs were compared with UEGs simulated by one of the most complete numerical models of the intact human heart currently available, during various stimulation modalities.

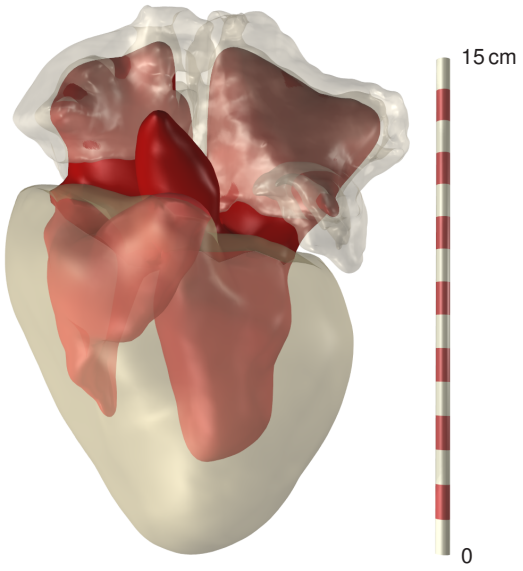

Figure 1: *Anatomy of the heart model used in this study. Ventricular and atrial cavities as well as the aorta were filled with blood. Atrial myocardium was included as a passive conductor.*

Materials and Methods

Action potentials were simulated with a large-scale computer heart model that has been described and validated previously [27, 38]. This model has anisotropic myocardium with transmurally rotating fiber orientation. Sinus rhythm was mimicked by stimulating the ventricles at the early activation sites published by Durrer et al. [12, 19]. Propagating AP were computed at 15 million points in the ventricular myocardium with a monodomain reaction-diffusion equation, based on ionic currents computed with the TNNP model for the human ventricular myocyte [37], which distinguishes endocardial, mid-myocardial, and epicardial cells. Differences between the left ventricle (LV) and right ventricle (RV) [11, 43] were implemented as detailed in table 1.

The anatomy of the model is illustrated in figure 1. The atria were not activated, but were included in the simulation of electrograms to allow the reference potential to be set to zero at the roof of the right atrium [27]. Ventricular and atrial cavities were filled with blood.

Two different models were used for the computation of electrograms: a "realistic model" and a "simple model."

realistic model

Let $V_m(\mathbf{x},t)$ be the membrane potential at time t and position $\mathbf{x}$ (boldface symbols are used to indicate vector quantities). The local UEG according to the realistic model, $\phi_e(\mathbf{x},t)$, was computed from V_m throughout the heart by solving the bidomain equation [27, 41] in the form of equation (9) given in the Appendix, with the additional condition that $\phi_e(\mathbf{y},t) = 0$ at the reference electrode site, $\mathbf{y}$, in the right atrium. By solving this equation, $\phi_e(\mathbf{x},t)$ was obtained at 35 million model points in the ventricular myocardium, atria, connective tissue, and intracavitary blood. Details of the solution methods used are given in previous work [27]. To allow analysis of temporal derivatives, error tolerance levels were chosen 100 times lower than previously reported [27]. To limit the consequent increase in computation time, we chose a lower spatial resolution of 0.25 mm for computation of both AP and electrograms. The resulting errors in propagation velocity were compensated by choosing 15 % higher values for the conductivity in the intracellular domain. Nominal conductivity values were taken from literature [31]. The adapted conductivities were $g_{eT} = 0.12$, $g_{eL} = 0.30$, $g_{iT} = 0.035$ and $g_{iL} = 0.33$ Siemens/m, with subscript 'e' for the extracellular domain, 'i' for the intracellular domain, 'T' for transverse, and 'L' for longitudinal. The intracavitary blood had conductivity 0.6, connective tissue and atrial myocardium 0.2 Siemens/m.

simple model

We define $S(\mathbf{x},t)$, the simple model for the UEG at a point $\mathbf{x}$ as a function of time t, as the difference between a position-dependent "local component," $L(\mathbf{x},t)$, and a position-independent "remote component," $R(t)$:

$$S(\mathbf{x},t) = L(\mathbf{x},t) - R(t) \tag{1}$$

The names of these components reflect that $L(\mathbf{x},t)$ is completely determined by local activity, while $R(t)$ is dominated by remote activity. The local component, $L(\mathbf{x},t)$, is defined as a scaled mirror image of the local membrane potential:

$$L(\mathbf{x},t) = -\frac{g_i}{g_i + g_e} V_m(\mathbf{x},t) \tag{2}$$

where g_e and g_i represent the conductivities of the extracellular and intracellular domains, respectively. For the simple model, these conductivities are assumed to be isotropic. The rationale for equation (2) is given in the Appendix. The remote component is obtained by comparison to $\phi_e(\mathbf{x},t)$ computed by the realistic model, as follows. First we compute a residual signal, $r(\mathbf{x},t)$, for each location

$$r(\mathbf{x},t) = L(\mathbf{x},t) - \phi_e(\mathbf{x},t). \tag{3}$$

This signal contains the effects of anisotropy, inhomogeneities, and tissue boundaries, but it is dominated

Table 1: *Selected parameters of the ionic model and APD of isolated cells.*

	LV epi	LV M	LV+RV endo	**RV M**	**RV epi**
G_{to} (nS/pF)	0.294	0.294	0.073	**0.504**	**0.882**
G_{Ks} (nS/pF)	0.245	0.062	0.245	**0.112**	**0.490**
APD (ms)	272	324	275	303	244

Parameter values that are different from the original TNNP model [37] are printed in bold type. The affected parameters are the maximal conductances of the transient outward current (G_{to}) and the slow delayed rectifier current (G_{Ks}) [37]. APD = action potential duration at steepest downstroke of the AP. APD was measured at 1000 ms cycle length. Units are nS = nanoSiemens, pF = picoFarad, ms = millisecond.

by the differential effect of activity throughout the myocardium on the positive (exploring) and negative (reference) electrodes. To single out the global effect, we take the average, $R(t)$, of $r(\mathbf{x}, t)$ obtained from a large number of different locations $\mathbf{x}$. We assume that local effects cancel out in averaging. We will show that $r(\mathbf{x}, t)$ from different sites are similar, so that approximating them by the average $R(t)$ has little effect on $S(\mathbf{x}, t)$ even if this assumption is incorrect. Alternatively, $R(t)$ can be computed directly from membrane potentials throughout the heart. A derivation based on lead field theory [14, 15, 20], is presented in the Appendix.

To facilitate the discussion, we introduce a signal V_R that can be compared to membrane potentials:

$$V_R(t) = -\frac{g_i + g_e}{g_i} R(t) \tag{4}$$

In the Appendix we demonstrate that $V_R(t)$ can be considered as a (weighted) average of $V_m(\mathbf{x}, t)$ over the surface that bounds the myocardium.

We now reformulate our definition of the simple model as follows:

$$S(\mathbf{x}, t) = -\frac{g_i}{g_i + g_e} [V_m(\mathbf{x}, t) - V_R(t)] \tag{5}$$

For the fraction $g_i/(g_i + g_e)$ the value 0.25 was chosen. This value is close to the ratio $g_{iT}/(g_{iT} + g_{eT})$ in the realistic model. This model is based on ideas that were independently published by Colli Franzone et al. [6] and by us [28], and is similar to a UEG model derived by Geselowitz [15] (see Appendix).

It is important to note that the two components of the simple model, L and R, have no direct physical meaning, i.e. they do not correspond to signals that can be observed independently. Only the difference between the two is meaningful.

statistics

The AP and UEG were analyzed at 10^4 randomly selected sites throughout the ventricular myocardium. From each simulated AP, repolarization time (T_R) and the instant of 90 % repolarization (T90) were determined and used as reference timings. T_R was defined as the instant of minimum first derivative (steepest downstroke) of the AP. In addition, the activation time T_A was defined as the instant of maximum first derivative (steepest upstroke) of the AP. Action potential duration (APD) was computed as $T_R - T_A$.

From the UEG at the same location we determined T_{up} and T_{down}, the instant of the T-wave apex (T_{apex}) [32], and the instant of minimum second derivative (T_{d2}), which has recently been reported to be related to T90 [5]. First, T-wave signs were determined. There is a continuous spectrum of positive, biphasic, and negative T waves in the UEG. To classify T waves as positive or negative, we evaluated the area under the electrogram, from 50 ms after the end of depolarization (the latest T_A) to the end of the simulation. A T wave was considered positive when the positive area exceeded the negative area. T_{up} and T_{down} were evaluated as the instants of maximum and minimum first derivative of the UEG, respectively, in the interval from 50 ms after the end of depolarization to the end of the simulation. For positive T waves, T_{down} was evaluated in the interval from T_{up} to the end of the simulation. The repolarization markers are illustrated in figure 2. Analysis of the UEG was the same for the Simple and Realistic models. All statistics were determined automatically by a computer program. No manual corrections were made.

Computation and analysis of ϕ_e and S was done at a 1-ms sampling rate. Therefore, timing results are expressed with 1-ms accuracy.

The difference between the realistic and simple UEGs at a site $\mathbf{x}$ was quantified using the relative difference

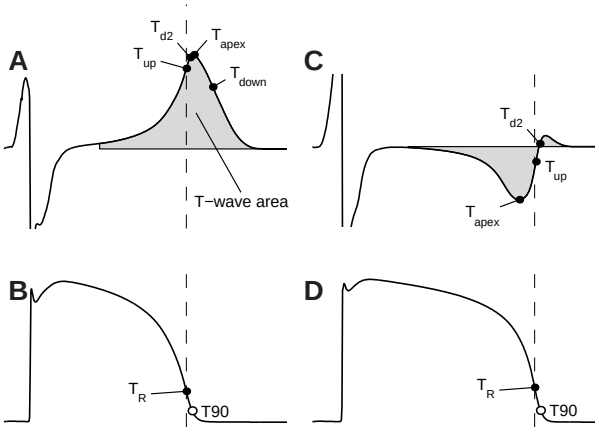

Figure 2: ***A,C:*** *Simulated UEG with illustration of the repolarization indices used; see text for their definitions.* ***B,D:*** *Simulated AP at the same locations as A and C, respectively, illustrating the reference markers. The dashed line in each panel marks the local T_R.*

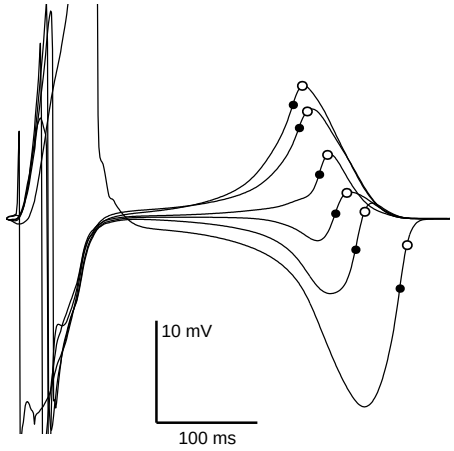

Figure 3: *Simulated UEGs (realistic model) from various sites in the ventricular myocardium. Local T_R are indicated with solid dots; local T90 with circles.*

(RD) [40] defined as

$$\mathrm{RD}(\mathbf{x}) = \sqrt{\frac{\sum_t (S(\mathbf{x},t) - \phi_e(\mathbf{x},t))^2}{\sum_t \phi_e(\mathbf{x},t)^2}} \qquad (6)$$

where the time index $t = 1, \ldots, 500$ ranges over all samples (depolarization and repolarization). The RD is a dimensionless measure of the difference between two signals (S and ϕ_e in our case); it is zero if the signals are identical.

Table 2: *Comparison of repolarization indices*

	positive T	negative T
N	4376 (44 %)	5624 (56 %)
$T_{up} - T_R$	-0.1 ± 2.3 ms	0.7 ± 1.8 ms
$T_{down} - T_R$	28.7 ± 8.1 ms	n.a.
$T_{d2} - T90$	-2.6 ± 1.4 ms	-2.5 ± 2.3 ms
$T_{apex} - T90$	2.8 ± 1.9 ms	-29.0 ± 10.7 ms

N = number of measurement locations.
Values are mean $\pm$ standard deviation.

Results

Predictions of the realistic model

To show the rationale for developing the simple model, we briefly review results obtained with the realistic model. These results summarize and expand previously reported findings [28, 29] and confirm results from studies with smaller-scale models [5, 6, 17, 34].

Figure 3 shows a representative sample of UEGs from the ventricular myocardium. Local repolarization times (T_R) are indicated with solid dots in the electrograms. These are invariably located on the upslope of the T wave.

In sinus rhythm, positive T waves were found in 44 % of the analyzed positions (table 2). Their average T_R was 40 ms earlier than that of negative T waves. In figure , panel A, T_R distribution is shown separately for positive and negative T waves. Clearly, positive T waves are generally associated with earlier repolarization than negative T waves. There is overlap between the distributions, reflecting the fact that repolarization time is associated with a continuous spectrum of T-wave configurations from entirely positive, through biphasic, to entirely negative. This is illustated in panel B of figure , using (signed) T-wave area as a single parameter to describe the configuration.

The performance of T_{up} in sinus rhythm is illustrated in figure , panel C. On 1000 points shown in the figure, 8 outliers are seen; the other points lie within a few milliseconds from the identity line.

The performance of T_{up}, T_{down}, T_{d2}, and T_{apex} on a sample of 10^4 randomly chosen sites throughout the ventricular myocardium, in sinus rhythm, is summarized in table 2. The table shows that T_{up} is a very accurate substitute for T_R. An alternative for T_{up} in positive T waves, T_{d2} predicts T90 reasonably well. In positive T waves, the performance of T_{apex} is similar to that of T_{d2} but with an opposite bias, whereas T_{down} performs very poorly.

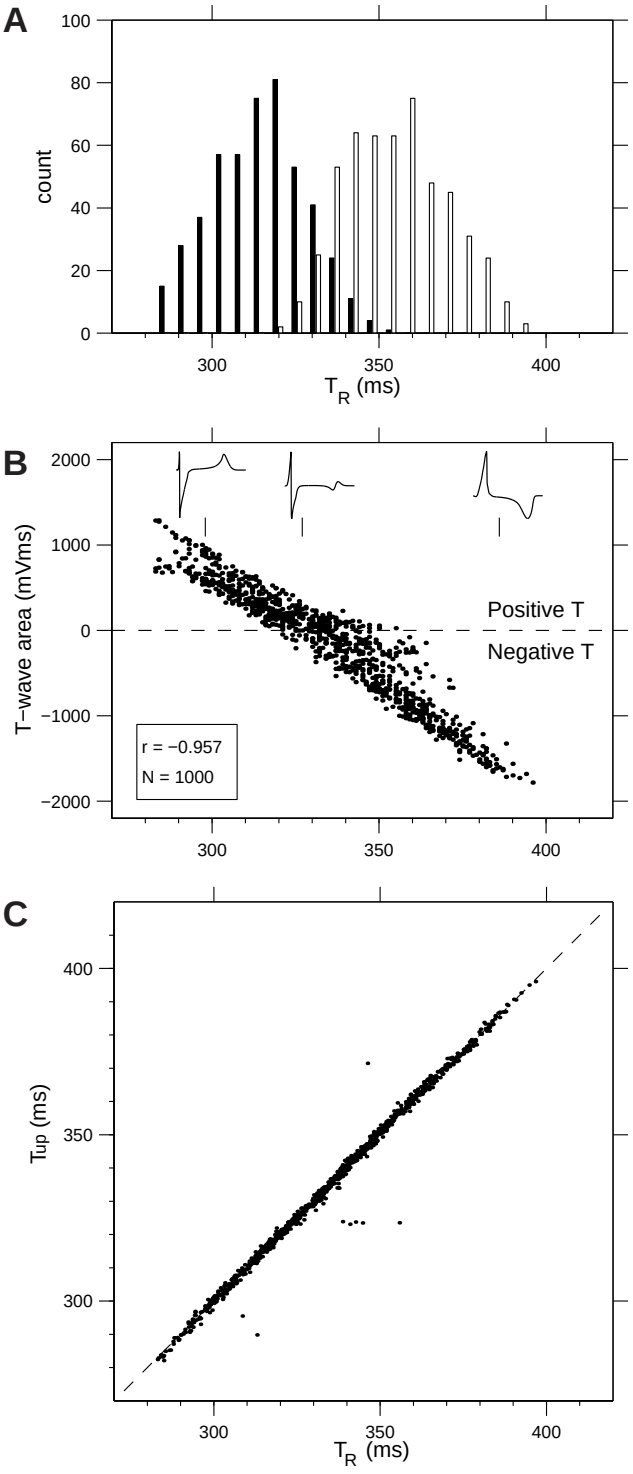

Figure 4: ***A:*** *Distribution of T_R for positive T waves (black bars) and for negative T waves (white bars); $N = 10^4$.* ***B:*** *scatter plot demonstrating the correlation between T_R and T-wave area; $N = 1000$. Three insets show typical UEGs whose T_R are indicated with vertical lines. The horizontal axis is the same as in panels A and C.* ***C:*** *scatter plot demonstrating the correlation between T_R and T_{up}; $N = 1000$.*

Pacing in the left ventricular apex caused repolarization to move predominantly from apex to base. This led to 85 % positive T waves and increased the difference in average T_R between positive and negative T waves to 70 ms. The accuracy of T_{up}, T_{down}, and T_{apex} as predictors for repolarization time was not affected (changes less than 1 ms). In a model with uniform intrinsic APD (all cells set to type endocardial; see table 1) 49 % of the T waves was positive and the difference in average T_R between positive and negative T waves was reduced to 31 ms (from 40 ms in sinus rhythm), but the accuracy of the repolarization indices was again not affected.

Remote component for the simple model

Residuals $r(\mathbf{x}, t)$ computed according to equation (3) for 100 randomly chosen myocardial sites are plotted in figure 5, panel A, together with their average. Although individual signals differ, the average gives a reasonable estimate of their individual shapes, especially during repolarization. To obtain a smooth signal, we used the average R from 10^4 randomly chosen sites to compute UEGs with the simple model.

Validation of the simple model

Examples of UEGs computed according to the simple model (equation 5) are shown in figure 5, panels B–E. These examples were chosen to illustrate a representative set of relative differences (RD) between the simple and realistic models. Figure 5, panel F, shows that the vast majority of the 1000 sampled sites had acceptable RD values. As expected with this highly simplified model, there were several bad matches as well. These typically occurred in thin trabeculae, where realistic UEGs have small amplitudes and are more influenced by remote activity. The simple model cannot account for this. The simple and realistic models agreed on the polarity of the T wave in 90 % of the analyzed positions ($N = 10^4$).

The performance of the simple model was similar for different activation and repolarization sequences. Whereas for sinus rhythm the median RD was 0.29 ($N = 1000$), it was 0.23 for apical pacing and 0.31 for left ventricular epicardial pacing. In a model with uniform intrinsic APD, the median RD was 0.32 for sinus rhythm.

Insights from the simple model

Figure 6 (upper two rows) shows how the UEG is constructed according to the simple model. The UEG is computed as the inverted and downscaled difference between V_m and V_R (equation 5); it is positive when V_m

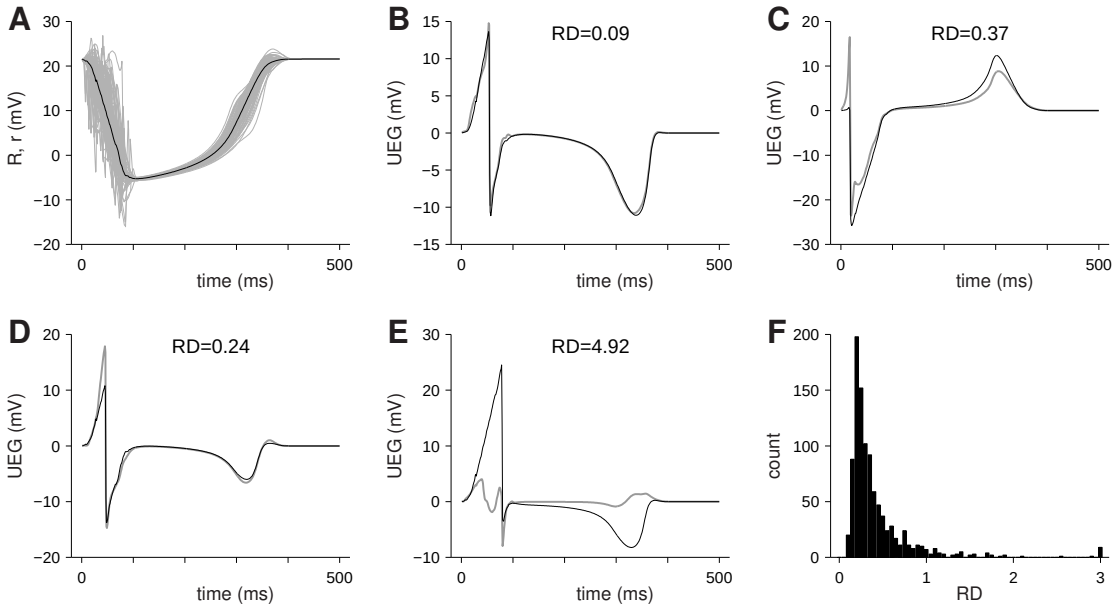

Figure 5: ***Panel A:*** *Determination of the remote component R. Gray lines: $r(\mathbf{x}, t)$ computed for 100 individual sites. Black line: average of these 100 signals.* ***Panels B–E:*** *UEG computed with the simple model (black) compared to the realistic model (gray). Positions were selected to show:* ***(B)*** *the best match;* ***(C)*** *a median match with positive T wave;* ***(D)*** *a median match with negative T wave; and* ***(E)*** *the worst match. The vertical axis gives potential (mV). Each panel gives the corresponding relative difference (RD).* ***Panel F:*** *frequency distribution of RD values over a sample of 1000 comparisons. The last bin represents RD $\geq$ 3.*

is more negative than V_R (blue area) and negative when V_m is more positive than V_R (red area). Thus, positive T waves must occur at early-repolarizing sites.

The third row of signals in figure 6 shows how the simple model compares to the realistic model.

The fourth row in figure 6 shows how the simple model can help us to understand the proposed repolarization indices T_up and T_down. It shows the temporal derivatives of the V_m and V_R signals. We will use the notation $\dot{V}$ to indicate the temporal derivative dV/dt. A dashed trace shows $\dot{V}_\mathrm{R}$ and a solid trace shows $\dot{V}_\mathrm{m}$. The minimum of $\dot{V}_\mathrm{m}$ defines T_R, which is indicated by a red vertical line. Coincident with this line is a dashed black vertical line, which indicates T_up, the instant of maximum $\dot{S}$. The (near) equality of T_R and T_up can be understood by observing that the maximum of $\dot{S}$, which is proportional to $\dot{V}_\mathrm{R} - \dot{V}_\mathrm{m}$, always occurs near minimum $\dot{V}_\mathrm{m}$, due to the soft slopes of V_R. Thus, in normal tissue, the remote component does not perturb T_up much.

The fifth row in figure 6 shows $\dot{S}$ itself. Its extrema, which define T_up and T_down, occur near the minima of V_m and V_R, respectively, but generally do not coincide exactly with these.

T_down occurs where the difference $\dot{V}_\mathrm{R} - \dot{V}_\mathrm{m}$ is most negative. At very early repolarizing sites (panel A in figure 6) T_down occurs well after the end of the local AP and corresponds with the minimum in $\dot{V}_\mathrm{R}$. At less early sites, it still occurs after the end of the AP, because $\dot{V}_\mathrm{R}$ can only dominate the difference when V_m is nearly back at resting potential. At sites with intermediate repolarization times, $\dot{V}_\mathrm{R}$ and $\dot{V}_\mathrm{m}$ together determine T_down. Both experimental [46] and numerical [28] studies have previously shown a (weak) correlation between T_down and repolarization time. However, a theoretical explanation has been lacking. The simple model readily explains this relation, also showing why it has a variable, non-unitary slope. According to the simple model, we should expect that for very early-repolarizing sites, where the downslopes of V_m and V_R occur far away from each other, the local component cannot influence T_down. Thus, at these sites T_down should be independent of T_R. At very late-repolarizing sites (panel C in figure 6), T_down is again very close to the minimum in $\dot{V}_\mathrm{R}$.

The T_d2 index can be understood by considering second-order derivatives, which correspond to curvature in the original V_m and V_R signals. T_d2 is defined as the instant of minimum $d^2\phi_\mathrm{e}/dt^2$, i.e. most down-

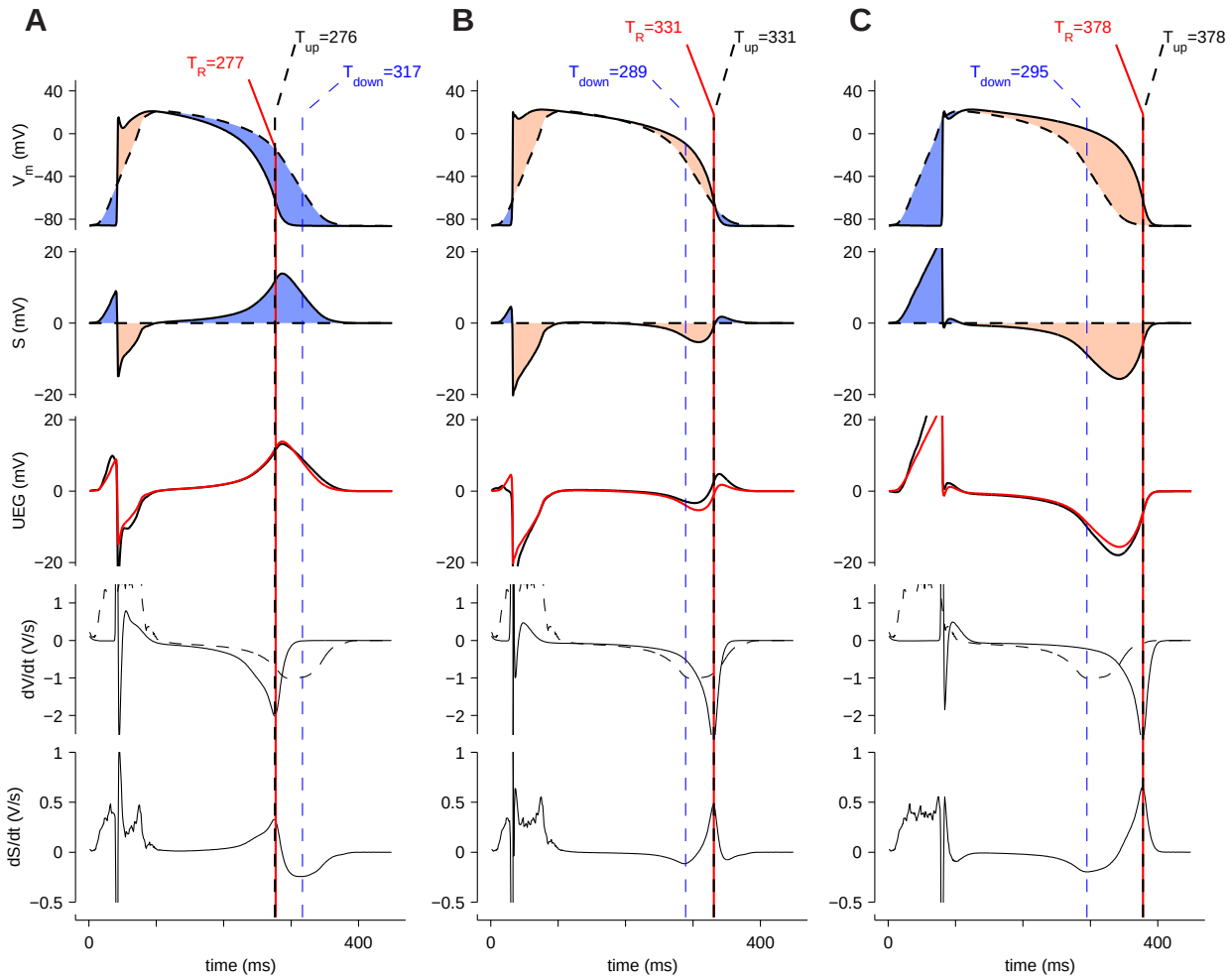

Figure 6: *Construction of UEGs with the simple model. The top frame in each panel shows simulated V_m from three different locations in the model (solid line) and the location-independent V_R (dashed). The second frame shows their downscaled and inverted difference, i.e. the UEG according to the simple model. In the third frame, this UEG (red) is compared to the UEG computed with the realistic model (black). The fourth frame shows the temporal derivatives $\dot{V}_m$ (solid line) and $\dot{V}_R$ (dashed). The fifth frame shows the temporal derivative of the UEG itself (computed with the simple model). Each red vertical line indicates T_R, i.e. the instant of minimum $\dot{V}_m$. Each of these lines is half obscured by a dashed black line which indicates T_{up}, leading to a black-red dashed line. Each dashed blue vertical line indicates T_{down}.* ***Panel A:*** *positive T wave.* ***Panel B:*** *biphasic T wave.* ***Panel C:*** *negative T wave.*

ward curvature in ϕ_e. According to the simple model, this corresponds to the most upward curvature in V_m, if distortion from V_R is negligible. This upward curvature occurs at the end of the AP, near T90 in healthy myocardium. Because V_R is a very smooth signal, its curvature is indeed negligible. This explains the small difference between T_{d2} and T90 (table 2). In positive T waves, the sharp turn in ϕ_e leads in most cases to the apex of the wave. Thus, in positive T waves, T_{apex} is close to T_{d2}.

We reported above that during apical pacing in the realistic model, 85 % of the myocardium showed positive T waves, while this was 44 % of sinus rhythm. The simple model explains this finding too. When the heart was paced at the apex, the basal region repolarized last. Because the reference electrode was near the base, this region was more strongly represented in V_R, and its late repolarization prolonged V_R. Since the majority

of sites now repolarized earlier than V_R, a majority of T waves became positive. During sinus rhythm positive T waves were a minority. An explanation for this is given in the Appendix: under the assumption that the myocardium is isotropic, only sites at the surface of the myocardium contribute to V_R. In the anisotropic heart this is not strictly true, but the surface still dominates. The fact that we used sites from the whole myocardium to determine V_R does not change this. Thus, the mid-myocardial region has less influence on V_R. In sinus rhythm, this region was the last to repolarize. Due to the small influence of this late-repolarizing tissue, repolarization of V_R during sinus rhythm occurred somewhat earlier than the average of the myocardium, making a larger volume of myocardium appear late-repolarizing and having negative T waves.

Although T_{up} and T_R are closely related, they do not coincide exactly. This can be understood in terms of the simple model as follows. In figure 7, the signals $\dot{V}_m$ and $\dot{V}_R$ are plotted in a short interval around T_R. These signals correspond to the first column in figure 6. In this case, T_R (the instant of minimum $\dot{V}_m$) was 277 ms and T_{up} (the instant of maximum $\dot{S}$) was 276 ms. The reason for this difference is that $\dot{S}$ is determined by both $\dot{V}_m$ and $\dot{V}_R$: From equation (5) it follows that $\dot{S}(\mathbf{x}, t)$ is proportional to $\dot{V}_R(t) - \dot{V}_m(\mathbf{x}, t)$. In the case of figure 7, the second derivative of V_m was smaller than the second derivative of V_R during a full sample interval before T_R, as shown by the tangent lines. Therefore, the difference $\dot{V}_R - \dot{V}_m$ was slightly larger at $t = 276$ ms than at $t = T_R$.

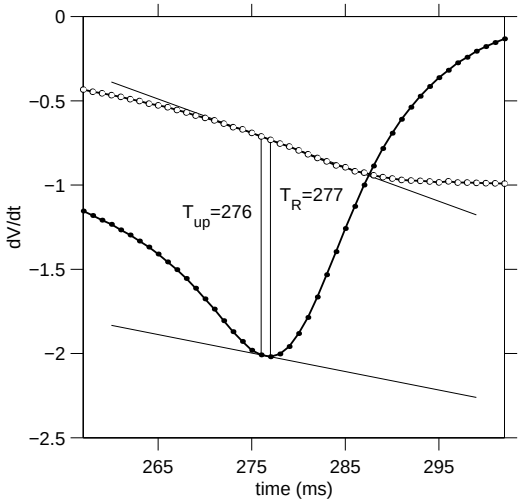

Figure 7: *Illustration of difference between T_{up} and T_R. The first derivative of the membrane potential, $\dot{V}_m$, at the same location as the leftmost column in figure 6, is shown with solid dots, connected with line segments (1-ms sampling interval). The signal $\dot{V}_R$ is shown similarly with open circles. Computed tangent lines to both signals at $t = T_R - 0.5$ ms demonstrate that the second derivative of V_R at this time is larger than the second derivative of V_m, leading to a difference of 1 ms between T_{up} and T_R.*

Discussion

We have shown that in healthy tissue the local contribution to the UEG is essentially a downscaled inverted AP. The electrogram is positive when local V_m is more negative than V_R. This explains why T waves are positive for early-repolarizing cells. Cells with intermediate repolarization times have a V_m that initially stays above V_R, but descends below it in the final stage of repolarization. This explains their biphasic T waves. As observed experimentally [8, 17], such biphasic waves always have a negative part followed by a positive part. In late-repolarizing regions the T wave is negative because the local membrane is still depolarized while it is repolarized elsewhere.

Due to the relatively soft slopes of V_R, first- and second-order derivatives of the UEG are dominated by the derivatives of V_m. Thus, where V_m makes its steepest descent, the UEG makes its steepest ascent. This explains the near-equality of T_{up} and T_R. Where V_m turns most sharply upward, the UEG turns most sharply downward. This explains the small difference between T_{d2}, T90, and, in positive T waves, T_{apex}. Only when V_m is very flat the slope of V_R can dominate the slope of the UEG. This leads to a coincidence of T_{down} and the instant of minimum dV_R/dt for very late- and very early-repolarizing sites. At sites with intermediate repolarization times, this relation is modulated by the slope of the local V_m, leading to a (weak) correlation between T_R and T_{down}.

The ARI and alternatives

Wyatt et al. proposed the activation-recovery interval (ARI) as a substitute for the APD, which cannot easily be measured in vivo [45]. The ARI was measured from the time of steepest downstroke of the UEG to the time of steepest upstroke of its T wave. Comparison with transmembrane APD and with effective refractory period demonstrated the validity of this method [3, 8, 17, 21]. A simulation study with a cable model also confirmed the method, and demonstrated some of the circumstances in which it is less accurate [34].

Other authors proposed that, for positive T waves, T_{down} should be used instead of T_{up} [2, 13, 46]. The original rationale for this "alternative method" was that in some studies its results correlated better with the du-

ration of the monophasic action potential [2, 46]. The intuition that the end of the local T wave (i.e. T_{down} for positive T waves) should correspond to local T_{R} may also play a role.

Our simple model shows that in normal tissue, T_{up} is temporally linked to T_{R}. This (simple) model is not suitable for all conditions. For example, it cannot faithfully simulate UEGs in case of fibrosis or intracavitary measurements. It is possible that the relation fails there, e.g. because the active tissue is so sparse or so far from the exploring electrode that the slope of V_{R} can dominate the slope of the UEG, or because the tissue is too anisotropic. However, it is difficult to imagine that under these conditions the relation between T_{R} and T_{up} would be replaced by a relation between T_{R} and T_{down}. Such circumstances can only be studied with a more realistic model [29].

Another possible alternative for T_{up} is the T-wave area, which correlates strongly with T_{R} [28, 42]. This relation may be useful as a last resort when T_{up} cannot be measured. However, caution is necessary because other factors may influence T-wave area. It may be a useful index if such problems can be ruled out, or in order to assess local changes in APD. When there is no opportunity for a quantitative analysis, the polarity of the T wave can give a coarse estimate of local repolarization time with respect to the average of the ventricular myocardium.

In model studies, T_{d2} too has shown potential as an estimate for T_{R} or T90, but its sensitivity to noise may limit its applicability in practice [5]. For positive T waves, T_{apex} is equally accurate.

Sources of inaccuracy in the ARI

Generally, T_{up} and T_{R} will not be exactly the same, because the UEG contains a remote component. At T_{R} itself, where $\dot{V}_{\mathrm{m}}$ is minimal, the second derivative of V_{m}, $\ddot{V}_{\mathrm{m}}$, is zero, so any signal component with a nonzero second derivative at T_{R} can modulate T_{up}. This displacement is limited to the interval in which the magnitude of $\ddot{V}_{\mathrm{m}}$ is smaller than that of the other components of the UEG. According to the simple model, the only other component is V_{R}. Its second derivative, $\ddot{V}_{\mathrm{R}}$, is generally small but not zero at T_{R}. If $\ddot{V}_{\mathrm{R}} < 0$ at T_{R}, T_{up} will be earlier than T_{R}, and if $\ddot{V}_{\mathrm{R}} > 0$ at T_{R}, T_{up} will be later than T_{R}.

In this study, the interval in which the absolute value of $\ddot{V}_{\mathrm{m}}$ is small enough to allow a difference between T_{up} and T_{R} was generally less than 2 ms long. However, in failing [30] or ischemic myocytes, the AP can have a long, linear downslope, i.e. a long interval in which the absolute value of $\ddot{V}_{\mathrm{m}}$ is small. This can lead to considerable differences between T_{up} and T_{R} [17, 34]. The same problem occurs with atrial myocytes that lack a plateau in their AP [42].

Other ways to explain the UEG

Previous explanations of the validity of the ARI were based on propagation in a uniform cable, which is equivalent to plane-wave propagation in a uniform isotropic 3-D medium [17, 34]. Under the assumption that the repolarization wavefront travels with a fixed velocity and the final phase of the AP is temporally symmetric about T_{R}, a strict equivalence of T_{up} and the instant of minimum third temporal derivative of V_{m} can be demonstrated [34]. A disadvantage of this approach is that the generalization to arbitrary repolarization sequences is not obvious.

Another UEG model that has been successful in providing insight is the oblique dipole layer [4]. Whereas this model is very useful in explaining anisotropic effects on the QRS complex, we think that it is not convenient for an explanation of the ARI and T-wave polarity.

The cable model can also be used to explain T-wave polarity. For depolarization wavefronts, this has been treated e.g. by Spach et al. [33]. With the signs inversed, this treatment is perfectly applicable to repolarization wavefronts. Just like the amplitude ratio of the R and S waves in the UEG contains information about depolarization time [10], the positive/negative amplitude ratio of the T wave gives information about repolarization time.

The remote component

The signal V_{R} was obtained in an ad-hoc way. In the Appendix, we argue that it can be interpreted as an average membrane potential. This average is not calculated over the entire myocardium, but only over its surface. In addition, different cells contribute to it with different weights, and these weights depend on the position of the reference electrode. This is to be expected, since the location of the reference is known to influence the UEG shape substantially. However, the amplitude of V_{R} is always similar to the AP amplitude, and its shape always represents a weighted average of remote AP.

Modeling techniques used

In our "realistic model," dispersion of AP shape was based on inhomogeneous expression of ion channels and subunits. Presently, these inhomogeneities are insufficiently characterized to explain the dispersion of AP shape in the human heart and to obtain normal T waves in the ECG [7, 36, 37]. However, the similarity of results obtained with the realistic model for different repolarization sequences demonstrates that a faithful represen-

tation of the true dispersion of AP shapes is not important for our study.

Conclusion

In normal myocardium, the UEG can be understood (approximately) as the difference between an inverted action potential and a remote component. With this simple model, the mechanism and limitations of all proposed repolarization markers can be readily explained. The relation between T_{up} and T_R, which has previously been established both theoretically and experimentally, can now be understood intuitively.

In positive T waves, there is a weak correlation between T_{down} and T_R. In contrast to the (near) identity relation between T_{up} and T_R, the relation between T_{down} and T_R has a variable, non-unitary slope. A theoretical basis for their correlation has been lacking. The simple model explains the correlation, and the non-unitary slope of the relation, making clear that this relation should not be exploited for the determination of repolarization times.

We confirm the conclusion that T_{up} is the best estimate of T_R, regardless of T-wave sign. T_{d2} and T_{apex} may sometimes be useful. T_{down} should never be used.

Grants

Computational resources for this work were provided by the Réseau québécois de calcul de haute performance (RQCHP).

This study was partially supported by the Netherlands Heart Foundation, grant nr. 2005B092.

M. Potse was partially supported by the Fonds de la recherche en santé du Québec (FRSQ), through the Research Center of Sacré-Coeur Hospital, Montreal, Quebec, Canada.

References

[1] Bayés de Luna A, Batchvarov VN, Malik M: The morphology of the electrocardiogram. In Camm AJ, Lüscher TF, Serruys PW, eds., *The ESC Textbook of Cardiovascular Medicine*. Blackwell Publishing, 2006.

[2] Chen PS, Moser KM, Dembitsky WP, Auger WR, Daily PO, Calisi CM, Jamieson SW, Feld GK: Epicardial activation and repolarization patterns in patients with right ventricular hypertrophy. *Circulation* 83: 104–118, 1991.

[3] Chinushi M, Tagawa M, Kasai H, Washizuka T, Abe A, Furushima H, Aizawa Y: Correlation between the effective refractory period and activation-recovery interval calculated from the intracardiac unipolar electrogram of humans with and without dl-sotalol treatment. *Jpn. Circ. J.* 65: 702–706, 2001.

[4] Colli-Franzone P, Guerri L, Viganotti C, Macchi E, Baruffi S, Spaggiari S, Taccardi B: Potential fields generated by oblique dipole layers modeling excitation wavefronts in the anisotropic myocardium; comparison with potential fields elicited by paced dog hearts in a volume conductor. *Circ. Res.* 51: 330–346, 1982.

[5] Colli Franzone P, Pavarino LF, Scacchi S, Taccardi B: Determining recovery times from transmembrane action potentials and unipolar electrograms in normal heart tissue. In Sachse FB, Seemann G, eds., *Proceedings of the Functional Imaging and Modeling of the Heart conference*, volume 4466 of *Lecture Notes in Computer Science*, pages 139–149. Springer, 2007.

[6] Colli Franzone P, Pavarino LF, Scacchi S, Taccardi B: Monophasic action potentials generated by bidomain modeling as a tool for detecting cardiac repolarization times. *Am. J. Physiol. Heart Circ. Physiol.* 293: H2771–2785, 2007.

[7] Conrath CE, Opthof T: Ventricular repolarization: An overview of (patho)physiology, sympathetic effects and genetic aspects. *Prog. Biophys. Mol. Biol.* 92: 269–307, 2006.

[8] Coronel R, de Bakker JMT, Wilms-Schopman FJG, Opthof T, Linnenbank AC, Belterman CN, Janse MJ: Monophasic action potentials and activation recovery intervals as measures of ventricular action potential duration: Experimental evidence to resolve some controversies. *Heart Rhythm* 3: 1043–1050, 2006.

[9] Coronel R, Opthof T, de Bakker JM, Janse MJ: The downslope of a positive T-wave of a local electrogram reflects remote activity. *Heart Rhythm* 4: 121, 2006. (letter).

[10] de Bakker JMT, Hauer RNW, Simmers TA: Activation mapping: Unipolar versus bipolar recording. In Zipes DP, Jalife J, eds., *Cardiac Electrophysiology: From Cell to Bedside*, pages 1068–1078. Saunders, Philadelphia, PA, second edition. 1994, ISBN 0-7216-4941-6: chapter 94.

[11] Di Diego J, Cordeiro J, Goodrow RJ, Fish JM, Zygmunt AC, Pérez G, Scornik F, Antzelevitch C: Ionic and cellular basis for the predominance of the Brugada syndrome phenotype in males. *Circulation* 106: 2004–2011, 2002.

[12] Durrer D, van Dam RT, Freud GE, Janse MJ, Meijler FL, Arzbaecher RC: Total excitation of the isolated human heart. *Circulation* 41: 899–912, 1970.

[13] Gepstein L, Hayam G, Ben-Haim SA: Activation-repolarization coupling in the normal swine endocardium. *Circulation* 96: 4036–4043, 1997.

[14] Geselowitz DB: On the theory of the electrocardiogram. *Proc. IEEE* 77: 857–876, 1989.

[15] Geselowitz DB: Description of cardiac sources in anisotropic cardiac muscle; application of the bidomain model. *J. Electrocardiol.* 25 Suppl., 1992.

[16] Gulrajani RM: *Bioelectricity and Biomagnetism*. New York, NY: Wiley, 1998. ISBN 0-47124-852-5.

[17] Haws CW, Lux RL: Correlation between in vivo transmembrane action potential durations and activation-recovery intervals from electrograms. Effects of interventions that alter repolarization time. *Circulation* 81: 281–288, 1990.

[18] Hodgkin AL, Rushton WAH: The electrical constants of a crustacean nerve fibre. *Proc. Roy. Soc. Lond. B* 133: 444–479, 1946.

[19] Lorange M, Gulrajani RM: A computer heart model incorporating anisotropic propagation: I. Model construction and simulation of normal activation. *J. Electrocardiol.* 26: 245–261, 1993.

[20] McFee R, Johnston FD: Electrocardiographic leads; I. introduction. *Circulation* 8: 554–568, 1953.

[21] Millar CK, Kralios FA, Lux RL: Correlation between refractory periods and activation-recovery intervals from electrograms: effects of rate and adrenergic interventions. *Circulation* 72: 1372–1379, 1985.

[22] Miller WT, III, Geselowitz DB: Simulation studies of the electrocardiogram; I. The normal heart. *Circ. Res.* 43: 301–315, 1978.

[23] Nagase S, Kusano KF, Morita H, Ohe T: Reply: Repolarization measurement in Brugada syndrome. *J. Am. Coll. Cardiol.* 52: 674–675, 2008. (letter).

[24] Plank G, Zhou L, Greenstein JL, Cortassa S, Winslow RL, O'Rourke B, Trayanova NA: From mitochondrial ion channels to arrhythmias in the heart: computational techniques to bridge the spatio-temporal scales. *Phil. Trans. Roy. Soc. A.* 366: 3381–3409, 2008.

[25] Plonsey R, Barr RC: Current flow patterns in two-dimensional anisotropic bisyncytia with normal and extreme conductivities. *Biophys. J.* 45: 557–571, 1984.

[26] Plonsey R, Fleming D: *Bioelectric Phenomena*. New York: McGraw-Hill, 1969.

[27] Potse M, Dubé B, Richer J, Vinet A, Gulrajani RM: A comparison of monodomain and bidomain reaction-diffusion models for action potential propagation in the human heart. *IEEE Trans. Biomed. Eng.* 53: 2425–2435, 2006.

[28] Potse M, Coronel R, Opthof T, Vinet A: The positive T wave. *Anatol. J. Cardiol.* 7 Suppl. 1: 164–167, 2007. (Proceedings of the 34th Int. Con. Electrocardiol.).

[29] Potse M, Coronel R, Opthof T, Vinet A: Simulating T-wave parameters of local extracellular electrograms with a whole-heart bidomain reaction-diffusion model: Size matters! In *Proc. 29th Annu. Int. Conf. IEEE EMBS*, pages 6644–6647, Lyon, France. 2007.

[30] Priebe L, Beuckelmann DJ: Simulation study of cellular electric properties in heart failure. *Circ. Res.* 82: 1206–1223, 1998.

[31] Roth BJ: Electrical conductivity values used with the bidomain model of cardiac tissue. *IEEE Trans. Biomed. Eng.* 44: 326–328, 1997.

[32] Savard P, Cardinal R, Nadeau R, Armour JA: Epicardial distribution of ST segment and T wave changes produced by stimulation of intrathoracic ganglia or cardiopulmonary nerves in dogs. *J. Auton. Nerv. Syst.* 34: 47–58, 1991.

[33] Spach MS, Barr RC, Serwer GA, Kootsey JM, Johnson EA: Extracellular potentials related to intracellular action potentials in the dog Purkinje system. *Circ. Res.* 30: 505–519, 1972.

[34] Steinhaus BM: Estimating cardiac transmembrane activation and recovery times from unipolar and bipolar extracellular electrograms: A simulation study. *Circ. Res.* 64: 449–462, 1989.

[35] Surawicz B, Saito S: Exercise testing for detection of myocardial ischemia in patients with abnormal electrocardiograms at rest. *Am. J. Cardiol.* 41: 943–951, 1978.

[36] Taggart P, Sutton PMI, Opthof T, Coronel R, Trimlett R, Pugsley W, Kallis P: Transmural repolarisation in the left ventricle in humans during normoxia and ischaemia. *Cardiovasc. Res.* 50: 454–462, 2001.

[37] ten Tusscher KHWJ, Noble D, Noble PJ, Panfilov AV: A model for human ventricular tissue. *Am. J. Physiol. Heart Circ. Physiol.* 286: H1573–H1589, 2004.

[38] Trudel MC, Dubé B, Potse M, Gulrajani RM, Leon LJ: Simulation of propagation in a membrane-based computer heart model with parallel processing. *IEEE Trans. Biomed. Eng.* 51: 1319–1329, 2004.

[39] van Oosterom A, Jacquemet V: Genesis of the P wave: Atrial signals as generated by the equivalent double layer source model. *Europace* 7 Suppl 2: S21–S20, 2005.

[40] van Oosterom A: Genesis of the T wave as based on an equivalent surface source model. *J. Electrocardiol.* 34 Suppl.: 217–227, 2001.

[41] Vigmond EJ, Weber dos Santos R, Prassl AJ, Deo M, Plank G, Bauer S: Solvers for the cardiac bidomain equations. *Prog. Biophys. Mol. Biol.* 96: 3–18, 2007.

[42] Vigmond EJ, Tsoi V, Yin YL, Pagé P, Vinet A: Estimating atrial action potential duration from electrograms. *IEEE Trans. Biomed. Eng.* , 2009. (published ahead of print).

[43] Volders PGA, Sipido KR, Carmeliet E, Spätjens RLHMG, Wellens HJJ, Vos MA: Repolarizing K^+ currents I_{TO1} and I_{Ks} are larger in right than left canine ventricular midmyocardium. *Circulation* 99: 206–210, 1999.

[44] Weiss DL, Seemann G, Dössel O: The end of T wave need not coincide with final repolarization in tissue: a simulation study. *Heart Rhythm* 4 Suppl.: S159, 2007.

[45] Wyatt RF, Burgess MJ, Evans AK, Lux RL, Abildskov JA, Tsutsumi T: Estimation of ventricular transmembrane action potential durations and repolarization times from unipolar electrograms. *Am. J. Cardiol.* 47 (Part II): 488, 1981. (abstract).

[46] Yue AM, Paisey JR, Robinson S, Betts TR, Roberts PR, Morgan JM: Determination of human ventricular repolarization by noncontact mapping; validation with monophasic action potential recordings. *Circulation* 110: 1343–1350, 2004.

[47] Yue AM: The controversy over measurement of activation recovery intervals continues. *Heart Rhythm* 4: 120–121, 2006. (letter).

[48] Yue AM: Repolarization measurement in Brugada syndrome. *J. Am. Coll. Cardiol.* 52: 674, 2008. (letter).

Appendix: Rationale for the Simple model

The bidomain model is the theoretical basis for almost all current modeling work in cardiac electrophysiology [14, 22, 24, 41]. It approximates the myocardium with two continuous domains. The "intracellular domain" represents the interior of myocytes and gap junctions, while the "extracellular domain" represents the interstitium. Intracavitary blood and connective tissue can be thought of as an extension of the extracellular domain [27]. The electric conductivity of each domain is represented by conductivity tensor fields $\mathbf{G}_\mathrm{i}$ and $\mathbf{G}_\mathrm{e}$, respectively. The bidomain model states that all current that leaves one domain at a given location must enter the other domain at the same location:

$$\nabla \cdot \mathbf{G}_\mathrm{i}(\mathbf{x}) \nabla \phi_\mathrm{i}(\mathbf{x}, t) = -\nabla \cdot \mathbf{G}_\mathrm{e}(\mathbf{x}) \nabla \phi_\mathrm{e}(\mathbf{x}, t) \qquad (7)$$

where ϕ_i and ϕ_e are the intracellular and extracellular potential fields. Using the transmembrane potential

$$V_\mathrm{m}(\mathbf{x}, t) = \phi_\mathrm{i}(\mathbf{x}, t) - \phi_\mathrm{e}(\mathbf{x}, t) \qquad (8)$$

the bidomain equation can be rewritten as

$$\nabla \cdot [\mathbf{G}_\mathrm{i}(\mathbf{x}) + \mathbf{G}_\mathrm{e}(\mathbf{x})] \nabla \phi_\mathrm{e}(\mathbf{x}, t) = -\nabla \cdot \mathbf{G}_\mathrm{i}(\mathbf{x}) \nabla V_\mathrm{m}(\mathbf{x}, t). \qquad (9)$$

This equation allows the computation of $\phi_\mathrm{e}(\mathbf{x}, t)$ from a known distribution of V_m. It only determines ϕ_e up to an arbitrary offset potential, which is fixed by defining $\phi_\mathrm{e}(\mathbf{y}, t)$ to be zero at the location, $\mathbf{y}$, of the reference electrode. Since (9) is an implicit equation which must be satisfied for all $\mathbf{x}$, it can only be solved in general by computing ϕ_e throughout the heart at once by solving a large system of linear equations [27]. The realistic model employed in this study uses this method. This solution process can not be intuitively understood. To arrive at an equation that can be easily understood, we assume $\mathbf{G}_\mathrm{i}$ and $\mathbf{G}_\mathrm{e}$ to be homogeneous and isotropic, so that we can represent them by scalars g_i and g_e and write

$$(g_\mathrm{i} + g_\mathrm{e}) \nabla^2 \phi_\mathrm{e}(\mathbf{x}, t) = -g_\mathrm{i} \nabla^2 V_\mathrm{m}(\mathbf{x}, t). \qquad (10)$$

In the absence of boundaries, the general solution of this equation is

$$\phi_\mathrm{e}(\mathbf{x}, t) = -\frac{g_\mathrm{i}}{g_\mathrm{i} + g_\mathrm{e}} V_\mathrm{m}(\mathbf{x}, t) + \phi_\mathrm{off}(t) \qquad (11)$$

where $\phi_\mathrm{off}(t)$ is an undefined offset potential [25]. Due to the assumption of isotropy, this equation for 3-D tissue is the same as the expression for ϕ_e in the one-dimensional cable [16, 18, 25]. The first term in equation (11) is our expression for the local component, $L(\mathbf{x}, t)$.

If we define the extracellular potential at a reference location, $\mathbf{y}$, to be zero: $\phi_\mathrm{e}(\mathbf{y}, t) \equiv 0$, we find the following expression for the offset potential:

$$\phi_\mathrm{off}(t) = \frac{g_\mathrm{i}}{g_\mathrm{i} + g_\mathrm{e}} V_\mathrm{m}(\mathbf{y}, t) \qquad (12)$$

Thus, bipolar electrograms can be computed with equation (11). For the UEG, a reference location in a passive medium (inactive tissue, blood, or perfusion fluid) must be used. This situation cannot be modeled realistically with an infinite-medium approach as used above. Therefore we seek to replace $\phi_\mathrm{off}(t)$ in equation (11) by a more general remote component $R(t)$ that can account for the inhomogeneities and boundaries of the body.

There are essentially two methods to compute UEGs in a bounded and inhomogeneous body. The first is to use a differential equation like (9). This is the approach taken by the realistic model used in this study. As stated above, it has the disadvantage of providing little insight in the mechanisms underlying the UEG. The second method is based on integral rather than differential expressions. A suitable integral-based method was proposed by Geselowitz in a brief conference paper [15]; details of his derivations are given in earlier work [14]. The method is based on what is now called an "equivalent double layer" [39]. Assume that a current I_app is injected through an exploring electrode at a point $\mathbf{x}$ inside the myocardium, and leaves through a reference electrode located at a point $\mathbf{y}$ outside the myocardium. The resulting current field inside the body, including the myocardium, is denoted as $\mathbf{J}_\mathbf{xy}$. The field $\mathbf{J}_\mathbf{xy}/I_\mathrm{app}$ is traditionally called the "lead field" [20] or "lead vector field" [26] for the given pair of electrodes. Assuming isotropic extracellular and intracellular media, the UEG, i.e., the potential difference between the two electrodes, $V_\mathbf{xy}$, can then be expressed as

$$V_\mathbf{xy} = -\frac{g_\mathrm{i}}{g_\mathrm{i} + g_\mathrm{e}} \left[V_\mathrm{m}(\mathbf{x}, t) + \frac{1}{I_\mathrm{app}} \int_S V_\mathrm{m} \mathbf{J}_\mathbf{xy} \cdot d\mathbf{S} \right] \qquad (13)$$

where S is the surface of the active myocardium, over which the product of V_m and $\mathbf{J}_\mathbf{xy}$ is integrated [15]. Comparison with equations (5) and (11) confirms the expression for the local component, $L(\mathbf{x}, t)$, and identifies the term involving the surface integral as what we named the remote component $R(\mathbf{x}, t)$ of the UEG. It is not obvious from this expression that R depends little on the position of the exploring electrode. Therefore we calculated lead fields $\mathbf{J}_\mathbf{xy}$ (using the same software as for the realistic model [27]) and evaluated the expression

$$R_{\mathbf{x}_n \mathbf{y}} = -\frac{g_\mathrm{i}}{g_\mathrm{i} + g_\mathrm{e}} \frac{1}{I_\mathrm{app}} \int_S V_\mathrm{m} \mathbf{J}_\mathbf{xy} \cdot d\mathbf{S} \qquad (14)$$

for five different positions $\{\mathbf{x}_n,\ n = 1 \ldots 5\}$ of the exploring electrode and a reference electrode at location $\mathbf{y}$

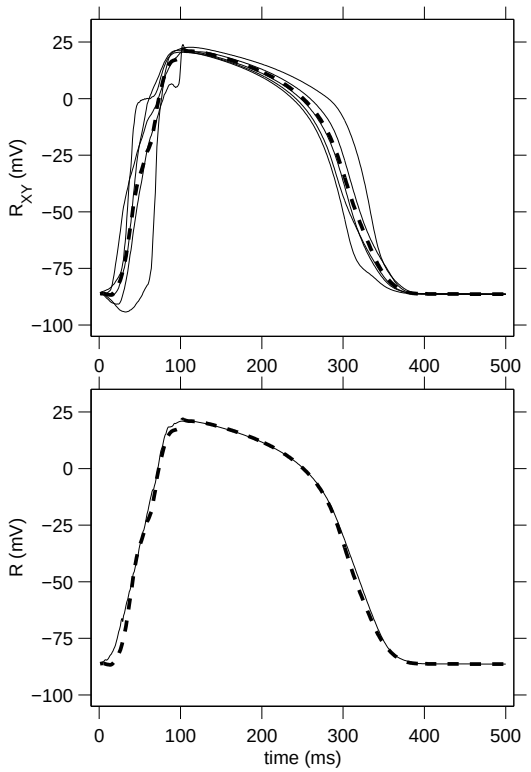

Figure 8: ***Panel A:*** *Thin solid lines show the remote component $R_{\mathbf{xy}}$ evaluated for a reference electrode in the left atrium and exploring electrodes (1) in the right ventricular subendocardium, (2) in the left-ventricular (LV) apical midmyocardium, (3) LV subendocardially in the tip of the septum, (4) LV basal subendocardial, and (5) LV posterior subepicardially at the level of the papillary muscles. The thick dashed line shows the average of these 5 signals.* ***Panel B:*** *The dashed line is the same as in panel A. The solid line is $R(t)$ according to the simple model (computed from residuals $r(\mathbf{x}, t)$ at many sites).*

in the left atrium. The results are shown in figure 8, and demonstrate that $R_{\mathbf{y}}$ defined as the average of several $R_{\mathbf{x}_n,\mathbf{y}}$ would be a good approximation for each individual $R_{\mathbf{x}_n\mathbf{y}}$. For practical reasons, R used elsewhere in this paper was obtained by subtracting the local component, $L(\mathbf{x}, t)$ from $\phi_e(\mathbf{x}, t)$ computed with a realistic model, and averaging the difference over many locations $\mathbf{x}$. Panel B of figure 8 shows that $R_{\mathbf{y}}$ and R are nearly identical. Since the purpose of our simple model is only to give insight, and not to replace the realistic model for numerical simulations, the actual method to arrive at R is not important.

From charge conservation, we must have

$$\int_S \mathbf{J}_{\mathbf{xy}} \cdot d\mathbf{S} = I_{\text{app}}. \tag{15}$$

Thus, equation (13) demonstrates that we can think of V_R for any pair of electrodes at $\mathbf{x}$ and $\mathbf{y}$, which can be expressed as

$$V_R = \frac{1}{I_{\text{app}}} \int_S V_m \mathbf{J}_{\mathbf{xy}} \cdot d\mathbf{S} \tag{16}$$

as an average membrane potential, albeit with a weighting that depends on the reference location. Under the assumption of isotropy, only V_m at the surface of the myocardium contributes. Therefore V_R does not reflect late repolarization of the mid-myocardium [44]. In the anisotropic heart, the deeper myocardium does contribute to V_R, but the surface still dominates.

In previous work we have computed V_R as a non-weighted average of V_m over the whole myocardium [28, 29]. The more general method employed here is more accurate, especially for abnormal repolarization sequences.

The simple model is not intended as an alternative for complete bidomain solutions, or competition for less crude approximations such as the oblique dipole model [4]. It is only a "rule of thumb" that allows us to explain how the UEG relates to action potentials. As such, it is similar to models that explain the electrocardiogram as a difference between two action potentials. Such models are used by many teachers of electrocardiography [1, 35].